

**OBSERVATION BASED ANALYSIS FOR OZONE PRODUCTION**

Lawrence I. Kleinman  
Atmospheric Sciences Division  
Brookhaven National Laboratory  
Upton, New York 11973-5000

Second Revision: May 2000

Published in  
Atmospheric Environment  
[vol. 34, 2023-2033 (2000)]

By acceptance of this article, the publisher and/or recipient acknowledges the U.S. Government's right to retain a nonexclusive, royalty-free copyright covering this paper.

This research was performed under the auspices of the United States Department of Energy under Contract No. DE-AC02-98CH10886.



PERGAMON

Atmospheric Environment 34 (2000) 2023–2033

ATMOSPHERIC  
ENVIRONMENT

www.elsevier.com/locate/atmosenv

## Ozone process insights from field experiments – part II: Observation-based analysis for ozone production<sup>☆</sup>

Lawrence I. Kleinman

*Environmental Chemistry Division, Brookhaven National Laboratory, Upton, NY 11973, USA*

Received 23 April 1999; accepted 11 September 1999

### Abstract

A complete characterization of O<sub>3</sub> photochemistry from a regulatory point of view includes knowing the production rate for O<sub>3</sub>, the sensitivity of this rate to NO<sub>x</sub> and VOCs, and the effects of emission controls on O<sub>3</sub> concentration. Observation-based analysis techniques have been developed to determine these quantities based on observed concentrations of O<sub>3</sub> and other photochemical ingredients. The promise of these methods is that reliable predictions on O<sub>3</sub> control measures will be forthcoming from easily made measurements. We review several techniques that have been used in recent field programs. Techniques are divided into two families according to whether predicted quantities pertain to the present state of an air parcel or to its history. The present time frame methods address the question of what is happening now, whereas the past time frame methods are used to determine how the air mass evolved to its present state. Present time frame methods are used to determine O<sub>3</sub> production rates and sensitivities. In this category, we discuss the constrained steady state, photostationary state, and radical budget methods. Past time frame techniques are used to address questions on the dependence of O<sub>3</sub> on precursor emissions. In this category, we discuss indicator species and the “observation-based model”. © 2000 Elsevier Science Ltd. All rights reserved.

*Keywords:* Ozone photochemistry; VOCs; Modeling

### 1. Introduction

We are able to measure most of the species that are important in the photochemistry that forms O<sub>3</sub>. A few species, such as the free radicals, OH, HO<sub>2</sub>, and RO<sub>2</sub>, are not yet routinely measured but progress is being made. Measurements by themselves, however, do not tell us all that we want to know about O<sub>3</sub> production. The most interesting quantities cannot be directly measured, not even in principal. Among these quantities are rates for the chemical production and loss of O<sub>3</sub> and other compounds. Most of all, we want to know the sensitivity of the atmosphere to changes in O<sub>3</sub> precursors; for example,

$d[\text{O}_3]/dE_{\text{NO}_x}$  and  $d[\text{O}_3]/dE_{\text{VOC}}$ , where  $E$ 's are emission rates of NO<sub>x</sub> (NO + NO<sub>2</sub>) and VOCs (broadly defined here to include CO).

These quantities can be obtained by running emission-based models in which O<sub>3</sub> production is calculated from first principles starting from emissions of precursor compounds. Another approach which has been developed in the last several years is that of “observation-based analysis” in which observed concentrations are used to make predictions on O<sub>3</sub> formation (Cardelino and Chameides, 1995). The general thrust of observational-based analysis is that by bringing in the actual atmospheric concentrations, there is less reliance on ill-characterized emissions, computational demands are lessened, and an element of reality is imposed on the problem.

In this article we review several observation-based analysis techniques that have been employed in recent field campaigns to obtain O<sub>3</sub> production rates and sensitivities in terms of quantities that can be measured. This

<sup>☆</sup>By acceptance of this article, the publisher and/or recipient acknowledges the U.S. Government's right to retain a nonexclusive, royalty-free copyright covering this paper. This research was performed under the auspices of the United States Department of Energy under Contract No. DE-AC02-76CH00016.

is a selective review with examples chosen to illustrate the present and past time frames that are used to describe  $O_3$  production. The present-time frame methods are directed at characterizing the current state of an air parcel including  $O_3$  production rate and the sensitivity of that rate to  $NO$  and  $VOCs$ . The past time-frame methods reach back into the history of the air parcel to determine the important pollutant control questions of how  $O_3$  was formed and what would happen if emissions were changed. Our examples include constrained steady-state box models, photostationary state, and radical budget methods for the present time frame; indicator species and the observation-based model (OBM) of Cardelino and Chameides (1995) for the past time frame. We focus on the varying methodologies and the relations between these methods.

The methods discussed here have been used for a wide range of applications. Some of the methods, such as the constrained steady-state box model calculation have long been a main stay in the analysis of data from atmospheric chemistry field experiments. Other methods are quite new and it is still an area of active research as to how these techniques can best be applied to making predictions on  $O_3$  formation.

## 2. Time scales

Two time scales must be considered: the present and the past. An important problem in applying observation-based techniques is how one should use information about the present state of an air mass to deduce what has happened in the past.

The “present” refers to the instantaneous chemistry that is occurring at the time and place where we make our measurements while the “past” refers to the history of the air mass. Examples of quantities that are uniquely defined by the present state of an air mass are chemical production and loss rates, and the sensitivities of these rates to changes in precursor concentration, i.e.  $dP(O_3)/d[NO]$  and  $dP(O_3)/d[VOC]$ , where  $P(O_3)$  is the chemical production rate of  $O_3$ . Examples of quantities that depend on the history of an air mass are  $d[O_3]/dE_{NO_x}$  and  $d[O_3]/dE_{VOC}$ . Note that these two derivatives are non-local. They represent the change in  $O_3$  concentration at a particular location due to an imposed change in emissions at some earlier time and some upwind region. Simply put, the present case models address the question “What’s happening now?”, while the past case models ask “How was the  $O_3$  formed?”.

The problem that we are faced with is that measurements are local – they are made at particular times and locations. It is therefore relatively easy to obtain information about the present, but difficult to obtain the emission control derivatives,  $d[O_3]/dE_{NO_x}$  and  $d[O_3]/dE_{VOC}$  which depend on the past history of the air mass. Thus,

instantaneous rates and sensitivities can be readily determined from steady-state box model calculations driven by observed concentration of stable species. Approximate methods such as radical budget and photostationary state approaches can also be used.

Observation-based answers to emission control questions must rely on other less rigorous approaches. A seminal contribution to this topic has been the idea that photochemical oxidation products carry with them a record of conditions during the past when ozone was being formed (Milford et al., 1994; Sillman, 1995; Sillman et al., 1998). By examining the concentrations of these end products or, better still, ratios of concentrations of end products, Sillman is able to predict whether  $O_3$  formation occurred under  $NO_x$  or  $VOC$ -limited conditions.

The method developed by Cardelino and Chameides (1995) is perhaps best described as a hybrid of present and past time-frame modeling. The emission control quantities (which relate to the past history) are determined from a sequence of present moment measurements.

## 3. Present time frame

Given a complete set of observations of stable compounds we can make a nearly exact calculation that completes the present moment characterization of an air mass. “Exact” in this context means that no approximations are made beyond those that are contained in the photochemical mechanism and those that are inherent in the measurement of input data. This, of course, is no guarantee of an accurate or even useful prediction if the mechanism or input data is seriously off. But under a plausible set of ground rules, it is the best that can be done. Photostationary state and radical budget methods are not exact, in the sense that some reactions are ignored as being of lesser importance and, in the latter case, a phenomenological rate constant is used. In this section we describe steady-state calculations and the approximate photostationary state and radical budget methods. Only a few examples are discussed; it is not possible to cover all of the interesting applications.

### 3.1. Steady-state calculations

Photochemical box models have been used in a variety of field programs to deduce concentrations of free radicals and  $O_3$  production rates and sensitivities in terms of the atmospheric mixture of stable, measured compounds. One way of doing these calculations is to constrain the concentrations of measured species to their observed values and integrate the photochemical equations to steady state. We will refer to this method as constrained steady state (CSS).

CSS calculations yield the concentrations of rapidly reacting species which are in equilibrium with the set of measured compounds. The rapidly reacting species usually include OH, HO<sub>2</sub>, RO<sub>2</sub>, and NO<sub>2</sub>. Depending on the application, slower reacting compounds such as H<sub>2</sub>O<sub>2</sub>, ROOH, and HCHO, can either be input data for the model or calculated. If we call the calculated variables  $X_i$  and the constrained variables  $C_x$ , then the steady-state equations have the form

$$dX_i/dt = P_i(X_i, C_x) - L_i(X_i, C_x), \quad (1)$$

where  $P_i$  and  $L_i$  are production and loss rates, respectively, for compound  $i$ . There is a differential equation for each of the species that are not measured. Integrating Eq. (1) to steady-state yields an equilibrium solution that satisfies the steady-state condition,  $dX_i/dt = 0$ :

$$P_i(X_i, C_x) = L_i(X_i, C_x). \quad (2)$$

An integration time of minutes is sufficient for steady state to be reached, if the only calculated species are free radicals and NO<sub>2</sub>. Production and loss rates for HCHO, other carbonyl compounds, and peroxides have time constants of hours to days and a correspondingly long integration period is required. Steady-state solutions for these compounds only make sense in regions where concentrations are not rapidly varying.

A steady-state solution as defined above is one in which each species concentration converges to a single value, independent of time. The steady-state concept can be extended to include diurnal variations (e.g., Davis et al., 1996; Jacob et al., 1996). In these calculations, solar intensity and the concentrations of some species have a prescribed diurnal dependence. Eq. (1) is integrated for a multi-day period until the calculation converges to a solution that does not change from one 24 h solar cycle to the next. This procedure gives more realistic results for slowly reacting species such as HCHO and peroxides which do not come into rapid equilibrium with the current solar intensity and chemical mixture. We will see later on, in the discussion of past time frame methods, how time-dependent constraints have been applied to the emission control problem.

The  $X_i$ 's calculated from Eqs. (1) and (2) can be used to determine the production and loss rates for the compounds that have been measured (O<sub>3</sub> for example). The net chemical rate of change is then given by

$$dC_x/dt = P_x(X_i, C_x) - L_x(X_i, C_x). \quad (3)$$

The total rate of change in the atmosphere will have contributions from chemistry and also from transport and emissions; deposition is often made part of the chemical term. If we denote the transport and emissions term as  $S_x$ , then the actual rate of change in the atmosphere (denoted by "D") is given by

$$DC_x/Dt = dC_x/dt + S_x. \quad (4)$$

Under some conditions it is reasonable to assume that  $C_x$  is not varying or varying only slowly. Then an estimate of  $S_x$  can be obtained:

$$S_x = -dC_x/dt. \quad (5)$$

Eq. (5) has been used to estimate emission rates. For example, Jacob and Wofsy (1988) have calculated emission rates of isoprene needed to explain the isoprene concentrations observed over the Amazon Forrest.

Most large field campaigns, at least in the last several years, have included a modeling component in which O<sub>3</sub> production rates are calculated based on measured concentrations (e.g. MLOPEX, Liu et al., 1992; CITE 3, Davis et al., 1993; ABLE 3B, Fan et al., 1994; PEM-West A, Davis et al., 1996; MLOPEX 2, Cantrell et al., 1996; Eisele et al., 1996; TRACE A, Jacob et al., 1996; TOHPE, McKeen et al., 1997). Typically, a calculation will use O<sub>3</sub>, CO, VOCs, NO, solar intensity, and meteorological parameters as input. Sometimes measurements of HCHO and peroxides are also available, which can then be used as input variables or used to verify model predictions.

With the development of instruments for measuring OH and peroxy radicals there is now the potential of testing the fast photochemistry in the models against observations (e.g., Cantrell et al., 1992,1993,1996,1997; Eisele et al., 1994,1996; Poppe et al., 1994; McKeen et al., 1997). These calculations have shown agreement on occasion but have also revealed many puzzling discrepancies which could represent missing observations, new chemistry, or inaccuracies in the radical measurements. However, the lack of agreement that has been noted for some remote clean areas should not be interpreted as a sign that more polluted regions will give still worse results (Poppe et al., 1994).

The sensitivity of  $P(O_3)$  to NO and VOCs can be obtained by comparing a base case calculation with one having a perturbed NO or VOC concentration. A finite difference formula yields the sensitivities,  $dP(O_3)/d[NO]$  and  $dP(O_3)/d[VOC]$ . There are also a variety of sophisticated techniques for generating an array of sensitivity information; showing how each of the model outputs vary if any of the model inputs are changed. In the following sections dealing with radical budgets and indicator species we will return to the  $P(O_3)$  sensitivities. For that purpose it is useful to define relative sensitivities:

$$d \ln P(O_3)/d \ln [C] = ([C]/P(O_3)) dP(O_3)/d[C]. \quad (6)$$

where  $C$  is either NO or VOC.  $d \ln P(O_3)/d \ln [C]$  has a value of 1 if an  $n\%$  change in  $[C]$  produces an  $n\%$  change in  $P(O_3)$ . The sensitivities in Eq. (6) look similar to the incremental reactivities used by Carter and Atkinson (1989) for the emission control problem, but note that all of the quantities in Eq. (6) are defined by the

instantaneous state of an air parcel. In contrast, incremental reactivities describe the sensitivity of current  $O_3$  to a change in precursor concentrations at an earlier time.

By definition we specify that  $O_3$  production is hydrocarbon or  $NO_x$  sensitive according to whether  $d \ln P(O_3)/d \ln[VOC]$  is larger than  $d \ln P(O_3)/d \ln[NO]$  or vice versa. The transition between  $NO_x$  and hydrocarbon limited conditions is a smooth one with systems near the transition point exhibiting an equal sensitivity to  $NO_x$  and VOCs.

### 3.2. Photostationary state

The so-called photostationary state (PSS) reactions establish a rapid equilibrium between  $O_3$ , NO, and  $NO_2$  (Leighton, 1961). Under many circumstances the departure from this equilibrium is due to  $O_3$  forming reactions which allows us to calculate  $P(O_3)$  in terms of readily observed quantities. The rapid photostationary state reactions are



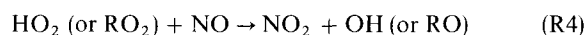
followed with nearly 100% yield by



These reactions constitute a do-nothing cycle as far as  $O_3$  production is concerned; R1 destroys as much  $O_3$  as R2–R3 makes. The resulting equilibrium is given by

$$j_{NO_2}[NO_2] = k_1[NO][O_3]. \quad (7)$$

This equilibrium is upset by the reactions that yield net production of  $O_3$ , namely



followed by R2–R3. Setting the production rate of  $NO_2$  equal to its destruction rate yields a steady state solution to R1–R4:

$$k_4([HO_2] + [RO_2])[NO] + k_1[NO][O_3] = j_{NO_2}[NO_2]. \quad (8)$$

The first term in Eq. (8) is  $P(O_3)$ , so rearranging gives

$$P(O_3) = j_{NO_2}[NO_2] - k_1[NO][O_3]. \quad (9)$$

Conditions under which Eq. (9) is valid have been discussed by Parrish et al. (1986) and Cantrell et al. (1993). The most important restriction is that the steady-state assumption applies, i.e. that the time rate of change of NO,  $NO_2$ , and  $O_3$  be near zero. Changing solar conditions due to clouds and changing  $NO_x$  concentrations due to local plumes can invalidate that assumption. Implicit in Eqs. (8) and (9) is the assumption that there are

not any other reactions that convert NO to  $NO_2$  or otherwise affect the NO to  $NO_2$  ratio (Parrish et al., 1986; Crawford et al., 1996). The assumption that  $HO_2$  and  $RO_2$  radicals react with NO with the same rate constant is discussed by Cantrell et al. (1997).

In the steady-state approach,  $P(O_3)$  depends on the entire set of photochemical reactions (including radical production, VOC oxidation, and peroxide formation) that determine the distribution and concentrations of peroxy radicals. There is a lot that can go wrong with such a calculation. The PSS method by-passes the detailed calculation of peroxy radicals by using Eq. (9) which express the fact that according to R1–R4, the effects of peroxy radicals are contained in the observed concentrations of NO,  $NO_2$ , and  $O_3$ .

There is a long history of attempts to apply the PSS equations using ambient NO,  $NO_2$ ,  $O_3$ , and solar intensity measurements. As a practical matter, it is difficult to get high accuracy predictions of  $P(O_3)$  from Eq. (9), because the form of that equation causes large error propagation (Kleinman et al., 1995; Cantrell et al., 1997). It is only in the last decade or so that measurements have become accurate enough to get useful chemical predictions. Another recent development is the ability to measure peroxy radicals which, when combined with NO measurements, yields an independent way of determining  $P(O_3)$  (Cantrell et al., 1993,1996,1997).

Similar to the CSS calculations, comparisons between the PSS approach and other methods sometimes agree and sometimes do not (Chameides et al., 1990; Ridley et al., 1992; Cantrell et al., 1993,1997; Davis et al., 1993; Kleinman et al., 1995; Crawford et al., 1996; Hauglustaine et al., 1996). Sometimes there is agreement on one day and not on the next. It is not clear at this point whether problems are mainly experimental or theoretical.

### 3.3. Radical budget

The simple conservation requirement that the formation rate of free radicals ( $OH + HO_2 + RO_2$ , also called odd-hydrogen) must equal their destruction rate can be used to derive approximate equations for  $P(O_3)$  and the sensitivity of  $P(O_3)$  to NO and VOCs (Sillman et al., 1990; Sillman, 1995; Kleinman et al., 1995,1997). Radical balance can be symbolically expressed as

$$Q = L_P + L_R + L_N \equiv 2P(\text{peroxide}) + L_R + P(NO_2), \quad (10)$$

where  $Q$  is the production rate of radicals (determined largely by photolysis reactions),  $L_P$  is the removal rate due to reactions forming peroxide,  $L_R$  is the removal rate due to other radical – radical reactions such as  $OH + HO_2$ , and  $L_N$  is the removal rate due to reactions between radicals and  $NO_x$ . In the second identity, the

loss rates for radicals are expressed in terms of the corresponding production rates of oxidation products. In general,  $L_R$  is small and will be ignored.

Under low  $\text{NO}_x$  conditions,  $L_N$  can also be ignored. Then production of radicals is equal to their removal by forming peroxides.

$$Q = 2k_5[\text{HO}_2]^2 + 2k_6[\text{HO}_2][\text{RO}_2], \quad (11)$$

where  $k_5$  and  $k_6$  are rate constants for



Eq. (11) can be solved for the total peroxy radical concentration,

$$[\text{HO}_2] + [\text{RO}_2] = 1/(2k_{\text{eff}})^{1/2}Q^{1/2}, \quad (12)$$

where the effective rate constant for forming peroxides,  $k_{\text{eff}}$ , is given in terms of the organic peroxy radical fraction,  $\alpha$ , by

$$k_{\text{eff}} = k_5(1 - \alpha)^2 + k_6(1 - \alpha)\alpha, \quad (13)$$

$$\alpha = [\text{RO}_2]/([\text{HO}_2] + [\text{RO}_2]). \quad (14)$$

$\alpha$  must be obtained elsewhere, i.e. from detailed calculations or estimated from experience in a similar environment.

Once the total peroxy radical concentration is available,  $P(\text{O}_3)$  can be calculated from (R4), yielding the low  $\text{NO}_x$  formula (Kleinman et al., 1995):

$$P(\text{O}_3) = k_4/(2k_{\text{eff}})^{1/2}Q^{1/2}[\text{NO}], \quad (15)$$

The utility of Eq. (15) is that it yields an estimate for  $\text{O}_3$  production rates in terms of quantities that can be readily measured.  $\text{NO}$  is required as explicitly shown in Eq. (15). A credible estimate for  $Q$  can be obtained from

$$Q = 2J(\text{O}_3 \rightarrow \text{O}^1\text{D})[\text{O}_3][\text{H}_2\text{O}] + 2J(\text{HCHO} \rightarrow 2\text{HO}_2)[\text{HCHO}], \quad (16)$$

where the  $J$ 's are photolysis rate constants depending on UV-solar irradiance and in the case of  $J(\text{O}_3)$  depending on the quenching rate of  $\text{O}^1\text{D}$ . Eq. (15) is relatively unaffected by "measurement" error as the least well-known quantities (including  $k_{\text{eff}}$ ) appear under a square root sign effectively halving the associated errors.

The CSS calculation offers several advantages over Eq. (15) in determining  $P(\text{O}_3)$ , but at the expense of requiring a more complete set of observations including  $\text{CO}$  and  $\text{VOCs}$ . Eq. (15) and the derivation leading up to it show how the additional information in the CSS calculation impacts the determination of  $P(\text{O}_3)$ . The CSS method provides an a priori determination of the distribution of

$\text{HO}_2$  and  $\text{RO}_2$  radicals which is equivalent to determining  $k_{\text{eff}}$  based on the ambient mixture of  $\text{VOCs}$  and their oxidation pathways. The CSS method can potentially provide concentration estimates for radical precursors that have not been measured thereby yielding a more accurate value for  $Q$ . Finally, the CSS method is not restricted to low  $\text{NO}_x$  situations. In the terminology used for Eq. (10), radical loss due to  $L_R$  and  $L_N$  is taken into account.

Low  $\text{NO}_x$  formulas have been used to determine  $P(\text{O}_3)$  in Metter, GA, a rural region in the southeastern US, and in the North Atlantic Ocean, near Yarmouth, Nova Scotia (Kleinman et al., 1995, 1998). In Metter, GA, comparison was made with  $P(\text{O}_3)$  determined from the photostationary state relations. These methods agreed to the extent expected based on uncertainty estimates. In Nova Scotia, comparison was made with  $P(\text{O}_3)$  calculated from a photochemical model that was constrained with observed concentrations. It was found that Eq. (15) captured 99% of the variance in  $P(\text{O}_3)$  from the model calculations. However, unlike the comparison with the PSS results, the constrained calculation does not represent an independent way for the calculation of  $P(\text{O}_3)$ . Agreement merely means that Eq. (15) has the right functional form to reproduce the "exact" model results in a low  $\text{NO}_x$  environment.

The radical budget equations can also be used to derive an approximate analytic formula for the relative sensitivities of  $P(\text{O}_3)$  to  $\text{NO}$  and  $\text{VOCs}$  (Kleinman et al., 1997). Because it is of interest to see how the sensitivities vary over a wide range of  $\text{NO}_x$  concentrations, the loss of radicals to reactions involving  $\text{NO}_x$ , (i.e.,  $L_N$ ) cannot be ignored. A general equation for  $P(\text{O}_3)$  is

$$P(\text{O}_3) = k_4/(2k_{\text{eff}})^{1/2}(Q - L_N)^{1/2}[\text{NO}], \quad (17)$$

where the terms have the same meaning as before. Relative sensitivities are obtained by differentiating Eq. (17) with respect to  $[\text{NO}]$  or  $[\text{VOC}]$ . An approximate formula giving the dependence of  $L_N$  on  $\text{NO}$  and  $\text{VOC}$  is based on Sillman (1995) and is provided in Kleinman et al. (1997). The relative sensitivities are given by

$$d \ln P(\text{O}_3)/d \ln[\text{NO}] = \frac{(1 - 3/2L_N/Q)}{(1 - 1/2L_N/Q)}, \quad (18)$$

$$d \ln P(\text{O}_3)/d \ln[\text{VOC}] = \frac{(1/2L_N/Q)}{(1 - 1/2L_N/Q)}. \quad (19)$$

The sensitivities are given in terms of a single independent variable,  $L_N/Q$ ; the fraction of radicals which are removed by reactions involving  $\text{NO}_x$ . While  $P(\text{O}_3)$  could be calculated readily from observation the same is not true for the sensitivities as  $L_N/Q$  is best determined from a steady-state photochemical calculation. The utility of Eqs. (18) and (19) is that they show very clearly the

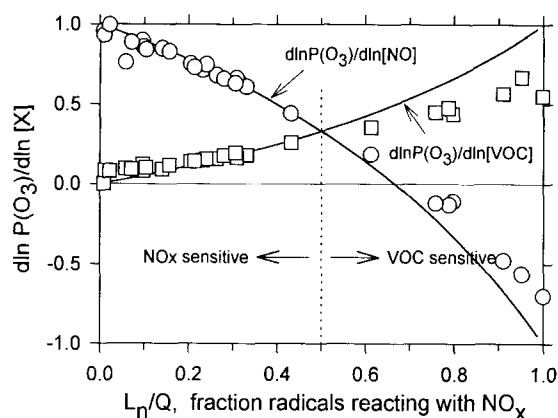


Fig. 1. The relative sensitivity of  $O_3$  production rate to  $[NO]$  and  $[VOC]$ ,  $d \ln P(O_3)/d \ln [NO]$  and  $d \ln P(O_3)/d \ln [VOC]$ , as a function of the fraction of radicals removed by reactions with  $NO$  or  $NO_2$ ,  $L_N/Q$ .  $P(O_3)$  is the chemical production rate of  $O_3$  and does not include destruction processes. Symbols are results from CSS calculations driven by observations from the Nashville urban area on 15 and 18 July, 1995 (adapted from Kleinman et al., 1997).

functional form of the solutions to a complex photochemical process and also provide a theoretical justification for one combination of indicator species.

Fig. 1 shows the dependence of  $d \ln P(O_3)/d \ln [NO]$  and  $d \ln P(O_3)/d \ln [VOC]$  on  $L_N/Q$ . Data points are from steady-state calculations constrained with observed values of  $O_3$ ,  $NO$ ,  $CO$ ,  $VOCs$ ,  $HCHO$ , and peroxides as measured from the DOE G-1 in the Nashville urban area during the summer 1995 SOS/Mid Tennessee field program (Kleinman et al., 1997). The analytic equations are seen to reproduce the qualitative features found in the “exact” CSS calculations. Curves in Fig. 1 while referring to instantaneous sensitivities have the same general features as found in the emission control problem (see e.g. Cardelino and Chameides, 1995).

Fig. 1 is separated into a  $NO_x$ -limited region and a VOC-limited region by a curve crossing that occurs at  $L_N/Q = 1/2$  (Sillman, 1995). When  $L_N/Q < 1/2$  the system is  $NO_x$ -limited and when  $L_N/Q > 1/2$  the system is VOC-limited. For  $L_N/Q > 2/3$ , the system is  $NO_x$  inhibited; increasing  $NO_x$  at this point results in a lower  $P(O_3)$ . According to Eq. (10), the conditions that  $L_N/Q$  be either less than or greater than  $1/2$  can be expressed as

$$2P(\text{peroxide}) > P(NO_2), P(O_3) \text{ is } NO_x\text{-limited,} \\ P(NO_2) > 2P(\text{peroxide}), P(O_3) \text{ is VOC-limited.} \quad (20)$$

According to the CSS results in Fig. 1,  $NO_x$  and VOC limits to  $P(O_3)$  are successfully predicted by Eq. (20).

The tendency to produce  $NO_2$  (specifically,  $HNO_3$ ) in VOC limited conditions and peroxides in  $NO_x$ -limited

conditions has also been analyzed by Tonnesen and Dennis (1997a). They showed numerically that  $O_3$  production rates are nearly proportional to the OH radical propagation efficiency,  $Pr_{OH}$  (the fraction of OH recreated for each OH that reacts), i.e.

$$P(O_3) \propto Pr_{OH} = f_{OH+VOC} Y_{HO_2/VOC} f_{HO_2+NO} \quad (21)$$

where the terms on the right-hand side describe three steps in the  $O_3$ -forming chain reaction.  $f_{OH+VOC}$  is the fraction of OH that reacts with VOC;  $Y_{HO_2/VOC}$  is the number of peroxy radicals created by  $OH + VOC$ ; and  $f_{HO_2+NO}$  is the fraction of peroxy radicals that react with  $NO$ . At high  $NO_x$ ,  $f_{OH+VOC}$  decreases because of reaction of OH with  $NO_2$  forming  $HNO_3$ . At low  $NO_x$ ,  $f_{HO_2+NO}$  decreases because of the formation of peroxides. The combination of these two “side” reactions causes a maximum in  $P(O_3)$  at a particular  $NO_x$  concentration. The ratio  $P(\text{peroxide})/P(HNO_3)$  is thereby an indicator of whether the atmosphere is on the low or high  $NO_x$  side of the  $P(O_3)$  maximum.

Tonnesen and Dennis (1997a) have argued that an effective  $O_3$  control strategy should include efforts to reduce  $P(O_3)$  in regions where it is high. They propose that  $NO_x$  and VOC limits to  $P(O_3)$  be determined from Eq. (21) using a measured set of “indicator” compounds including peroxy radicals,  $O_3$ , and  $NO$ . We will have more to say about indicator compounds in relation to past time frame problems.

#### 4. Past time frame

The formulation of an  $O_3$  control strategy requires that we know the emission control derivatives,  $d[O_3]/dE_{NO_x}$  and  $d[O_3]/dE_{VOC}$ , which give the response of  $O_3$  to changes in emissions of  $NO_x$  and VOCs. In contrast to the instantaneous sensitivities described above, the emission control derivatives are not properties of an air mass but rather depend on the entire sequence of events from the time that the  $NO_x$  or VOC was emitted to the time that the  $O_3$  is measured. These quantities are usually determined with an emission-based model by simply changing the emissions rates and seeing how  $O_3$  responds. There are, however, attractions to determining these quantities (more or less) directly from field observation, not the least of which is an enforced consistency with actual atmospheric concentrations.

One way of approaching this problem is to look for “indicator” compounds which maintain a record of whether  $O_3$  was formed under  $NO_x$  or VOC limited conditions (Sillman, 1995; Tonnesen and Dennis, 1997a,b). Another approach (the “OBM”) is to use a time sequence of observations to guide a photochemical calculation, which can then be repeated with perturbed

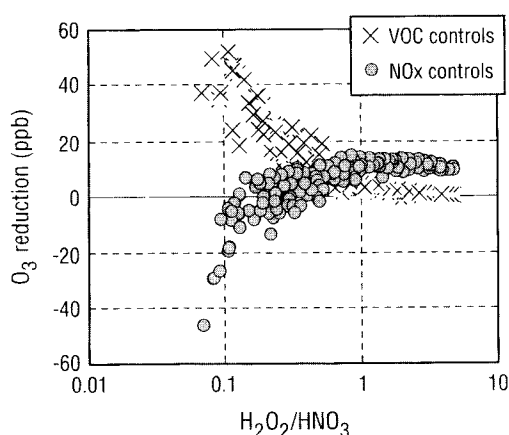


Fig. 2. Change in peak  $O_3$  concentration caused by either a 35% reduction in anthropogenic VOC emissions or a 35% reduction in  $NO_x$  emissions. Independent variable is the ratio of  $H_2O_2$  to  $HNO_3$  at the same point as the  $O_3$ . Results are from a 3-D Eulerian model simulation of the Lake Michigan area (adapted from Sillman, 1995).

emission rates (Cardelino and Chameides, 1995). In our terminology of present and past time frames, the indicator species approach uses a present moment observation to look back to the past. The OBM approach uses a sequence of present time-frame observations to reconstruct the time history of the air mass.

#### 4.1. Indicator species

Reactions that form  $O_3$  also yield oxidation products that can be used to determine whether  $O_3$  was formed under  $NO_x$ -limited or VOC limited conditions. The justification for this procedure is largely empirical but is backed up by theoretical reasoning related to the calculation of instantaneous sensitivities. As a matter of definition we note that  $NO_x$  is  $NO + NO_2$ ,  $NO_z$  is the sum of all of the oxidation products formed from  $NO_x$ , and  $NO_y = NO_x + NO_z$ .

#### 4.2. Peroxide – $NO_z$ ratio

The empirical approach is illustrated in Fig. 2 adapted from Sillman (1995). This figure, which was generated from Eulerian model output, shows the reduction in peak  $O_3$  concentration resulting from a 35% reduction in the emission rate of either  $NO_x$  (solid circles) or anthropogenic VOC (crosses). Ozone reduction is plotted as a function of the indicator ratio  $H_2O_2/HNO_3$ , determined at coincident points. Points that have a higher  $O_3$  reduction for  $NO_x$  controls are said to be  $NO_x$ -limited; if VOC controls produce a higher  $O_3$  reduction, then the system is VOC-limited. Points lie along two

reasonably well-defined curves. VOC-limited conditions are predicted by the model to go along with low values of the ratio  $H_2O_2/HNO_3$ , while  $NO_x$ -limited points are associated with high values of this ratio. Because there is some scatter in the calculated points, there is a range of indicator ratios which could be associated with either  $NO_x$ - or VOC-limited conditions. The particular value at which the  $NO_x$  and VOC curves cross (in the model and in the real world) depends somewhat on conditions such as deposition velocities and biogenic emission levels.

The theoretical justification for using  $H_2O_2/HNO_3$  as an indicator is given in Eqs. (18)–(20). Note that these equations explain  $NO_x$  and VOC limitations for  $P(O_3)$  in terms of  $P(\text{peroxide})/P(NO_z)$ , i.e. the theory explains present time frame sensitivities, not the sensitivity of  $O_3$  to emissions. However, it does seem plausible that the two problems are related as  $O_3$ ,  $NO_z$ , and peroxide concentrations are due to production occurring over the time history of an air mass.

Chemical production is not the only process that must be taken into account, as Trainer et al. (1993) note in their discussion of  $O_3/NO_z$  ratios. Other atmospheric processes that could effect the indicator ratios include mixing, deposition and chemical loss. The Eulerian model calculations take these processes into account so the empirical correlations are to be preferred over those that come out of an incomplete theory. Because chemical loss, deposition, and transport can vary from one problem to another there will always be some indeterminacy in relating indicator ratios to  $NO_x$  and VOC limitations. Time scales must also be carefully considered. The usefulness of indicator species is that they have a memory of conditions during the time period that  $O_3$  was formed. Deposition and chemical loss tend to erase this memory and impose a time window for viewing the past.

#### 4.3. $O_3 - NO_z$ ratio

Another family of indicator ratios consists of  $O_3/NO_z$  and variants constructed by subtracting background concentrations or by replacing  $NO_z$  with  $HNO_3$  or  $NO_y$ . In the absence of loss processes,  $\Delta O_3/\Delta NO_y$  is the number of molecules of  $O_3$  formed per  $NO_x$  molecule emitted.  $\Delta O_3/\Delta NO_z$  takes into account partial reaction of emitted  $NO_x$  as it is the number of  $O_3$  formed per  $NO_x$  consumed.

High values of the ratio  $O_3/NO_z$  are associated with  $NO_x$ -limited conditions and low values associated with VOC-limited conditions. A qualitative explanation for these tendencies was given by Sillman (1995). He noted that  $O_3$  photolysis is often the primary source of free radicals. In as much as the production rate of free radicals must equal their removal rate,

$$P(NO_z) + 2P(\text{peroxide}) = \alpha[O_3], \quad (22)$$

where  $\alpha$  is a proportionality constant that depends on solar intensity and water vapor concentration. Assuming that the  $\text{NO}_2$  concentration is proportional to its production rate (with proportionality constant  $\beta$ ) we get

$$[\text{O}_3]/[\text{NO}_2] = \alpha^{-1}(P(\text{NO}_2) + 2P(\text{peroxide}))/\beta P(\text{NO}_2). \quad (23)$$

Thus, the indicator ratio  $\text{O}_3/\text{NO}_2$  is rationalized in terms of the same instantaneous rates that were used to explain the connection between the ratio  $[\text{peroxide}]/[\text{NO}_2]$  and emission control strategies. The qualitative tendencies expected from Eq. (23) are in agreement with the modeling results of Lin et al. (1988), namely that there is a nonlinear relation between  $\text{O}_3$  and  $\text{NO}_y$ , such that the ratio increases in cleaner air (i.e.  $P(\text{peroxide}) \gg P(\text{NO}_2)$  at low  $\text{NO}_x$ , in clean air).

Eq. (23) is only qualitatively useful. Ultimately, predictions of  $\text{NO}_x$  and VOC limitation must be justified on empirical grounds. One approach, followed by Johnson and colleagues (Johnson, 1984; Johnson and Azzi, 1992) has been to use smog chamber data to develop an algorithm that yields predictions based on observed  $\text{O}_3$ ,  $\text{NO}_y$ , and  $\text{NO}_x$  concentrations. The resulting integrated empirical rate model and a revised method (Blanchard et al., 1998) that takes into account the nonlinear behavior seen by Lin et al. (1988) were developed independently of the indicator species approach, but appear to be functionally related. Sillman (1995) has used Eulerian model calculations to determine the values of the ratio  $\text{O}_3/\text{NO}_2$  that indicate whether  $\text{O}_3$  is  $\text{NO}_x$ - or VOC-limited. The procedure is the same as illustrated in Fig. 2 for deriving transition values for the ratio, peroxide/ $\text{NO}_2$ .

Part of the attraction in using  $\text{O}_3/\text{NO}_2$  is that it is easier to measure than peroxide/ $\text{NO}_2$ . Also, as first noted by Trainer et al. (1993), field measurements in many locations have revealed a very high correlation between  $\text{O}_3$  and  $\text{NO}_2$ , suggesting a causal relation. However, caution must be used in interpreting these ratios as the previous discussion on deposition, chemical loss, and time windows for viewing the past applies also to  $\text{O}_3/\text{NO}_2$ .

#### 4.4. Applications

Indicator species ratios have been used to analyze  $\text{O}_3$  production in Los Angeles, New York, Nashville, and Atlanta (Sillman et al., 1997,1998). These cities span a range of environments from VOC limited in Los Angeles to transitional in Nashville to  $\text{NO}_x$  limited in Atlanta as determined either from measured ratios or from Eulerian model calculations. Staffelbach et al. (1997a,b) used observed indicator ratios and a photochemical plume model to predict the sensitivity of  $\text{O}_3$  to  $\text{NO}_x$  and VOCs in southern Switzerland, downwind of the Milan urban plume. The integrated empirical rate

model, in its original form and modified for nonlinear behavior, has been used to predict  $\text{NO}_x$ - and VOC-limited conditions starting with routine monitoring data from several US cities (Chang and Suzio, 1995; Blanchard et al., 1998).

#### 4.5. Observation-based model (OBM)

Cardelino and Chameides (1995) have developed an approach that uses a sequence of present time-frame measurements to determine a response to perturbed emission rates. The first step in this calculation is to run a time-dependent model with concentrations of  $\text{O}_3$ , CO, NO, and VOCs constrained to their time-dependent observed values. This procedure can be viewed as a time dependent analogue of the CSS calculation discussed above (see Eq. (1)). This calculation yields a time-dependent solution for radicals and other substances which were not measured. The next step is to solve for the atmospheric source terms using Eq. (4):

$$S_z(t) = \text{DC}_z(t)/\text{Dt} - P_z(X_i, C_z, t) + L_z(X_i, C_z, t), \quad (24)$$

where  $P_z$  and  $L_z$  are determined from measured  $C_z$  and calculated  $X_i$ .  $\text{DC}_z(t)/\text{Dt}$  is the actual rate of change of compound  $z$  and is determined directly from a time series of measurements. A question arises as to how  $S_z$  should be interpreted since it is in part due to emissions and part due to transport. Cardelino and Chameides argue that the transport term is ultimately dependent on emissions and therefore  $S_z$  is a reasonable surrogate for the emissions that impact the measurement site. At this point they have characterized the time-dependent problem, including emission inputs. The next steps are to apply a perturbation to the  $\text{NO}_x$  or VOC emissions, repeat the time-dependent calculation without any constraints, and see how  $\text{O}_3$  responds. The method as actually implemented was somewhat more complicated than described above due to the necessity to account for vertical mixing.

Fig. 3 illustrates an application of an OBM to the Atlanta, GA urban area (Cardelino and Chameides, 1995). The effectiveness of reducing  $\text{O}_3$  by controlling  $\text{NO}_x$ , total VOCs, or anthropogenic VOCs is given by the corresponding relative incremental reactivity (RIR). The RIRs are the past time-frame analogues of the instantaneous relative sensitivities shown in Fig. 1. In this instance,  $\text{O}_3$  in Atlanta shows an almost equal sensitivity to  $\text{NO}_x$  and VOC reductions. At lower  $\text{NO}_x$  factors,  $\text{O}_3$  production becomes more  $\text{NO}_x$  sensitive; at higher  $\text{NO}_x$  factors more VOC sensitive. Controlling anthropogenic VOCs by themselves, however, does little to reduce  $\text{O}_3$ . At the point where the  $\text{NO}_x$  and total VOCs curves cross, the calculated indicator ratio,  $\text{H}_2\text{O}_2/\text{HNO}_3$ , has a value of 0.5, close to the curve crossing value shown in Fig. 2.

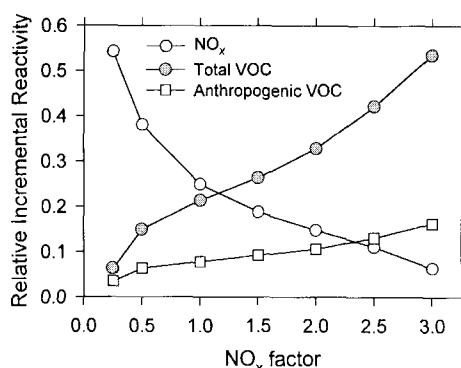


Fig. 3. Results from an OBM calculation of O<sub>3</sub> production in Atlanta, GA (W. Chameides, personal communication). Calculation is driven by average concentrations observed at six monitoring sites during a Southern Oxidants Study field program. Relative Incremental Reactivity is the percent change in O<sub>3</sub>, produced in the urban area, caused by an imposed percent change in the source term of the O<sub>3</sub> precursor. NO<sub>x</sub> factor = 1 is the actual NO<sub>x</sub> emission rate deduced by the OBM. Other NO<sub>x</sub> emission factors are for hypothetical situations with lower or high NO<sub>x</sub> emissions.

## 5. Conclusions

The common feature of the observation-based analysis techniques reviewed here is that they are used to translate field observations into information on O<sub>3</sub> production. We have divided the techniques into two categories according to whether the method provides information on the present state of an air parcel or on its history. In the former case, we are interested in knowing O<sub>3</sub> production rates and their sensitivity to NO<sub>x</sub> and VOCs, while in the latter case we are interested in the dependence of O<sub>3</sub> on emissions that occurred at some point in the past. Present time-frame methods included in this review are constrained steady state, photostationary state, and radical budget methods. Past time-frame methods are indicator species and “observation-based model”.

Because measurements are inherently local it is easier to obtain information about the present state of an air parcel than to determine its history. In the present time frame, the CSS method is a standard by which other methods can be judged as it potentially uses a full photochemical mechanism and a full suite of observed compounds to determine free radical concentrations and rates. In contrast past time-frame methods require significant approximations and an empirical justification that is obtained by comparisons with emission-based models.

Although the CSS method is “exact” in the sense of not requiring any significant approximations this is no guarantee that it is accurate. Recent field programs have

provided extensive data sets including OH and peroxy radical measurements against which CSS predictions can be tested. We briefly noted that CSS predictions and direct observations sometimes agreed and sometimes disagreed. This may indicate a faulty understanding of the photochemistry or a problem with the measurements. Where discrepancies exist, a significant effort has been made in finding the causes. It is outside of the scope of this review to evaluate these discrepancies but we note the importance of this problem.

Approximate methods for determining O<sub>3</sub> production rates and sensitivities include photostationary state and radical budget. The PSS technique is in many ways independent of the CSS method and thereby is a useful tool for checking CSS calculations and peroxy radicals measurements. The radical budget approach provides estimates of P(O<sub>3</sub>) based on a minimal set of observations. It is not independent of the CSS method but instead provides a compact description of the essential features of the O<sub>3</sub>-forming reactions. Relative sensitivities derived from the radical budget equations provide a qualitative justification for the use of indicator species.

Two approaches have been developed for determining past time-frame emission control information from present time-frame observations. The indicator species approach of Sillman (1995) depends on photochemical oxidation products carrying with them a record of past conditions during the time that O<sub>3</sub> was formed. The OBM of Cardelino and Chameides (1995) reconstructs the dependence on emissions from a sequence of present time-frame observations. The indicator species approach has the advantage of requiring only a point measurement of a pair of species such as H<sub>2</sub>O<sub>2</sub> and NO<sub>z</sub>. It yields a prediction of whether O<sub>3</sub> is NO<sub>x</sub>- or VOC-limited. Data requirements for the OBM are more extensive; a time series of observations of O<sub>3</sub>, NO, CO, and VOCs are required. This method yields quantitative predictions on the response of O<sub>3</sub> to changes in NO<sub>x</sub> and specific VOCs. Comparisons with Eulerian model results indicate that both methods are promising for evaluating emission controls.

## Acknowledgements

We gratefully acknowledge the continuing support of the Atmospheric Chemistry Program within the Office of Biological and Environmental Research of DOE under whose auspices we have conducted field programs and have developed some of the data analysis techniques described here. We also gratefully acknowledge support from R. Dennis of EPA to participate in the NARSTO Ozone Assessment. This research was performed under sponsorship of the US DOE under contracts DE-AC02-76CH00016.

## References

- Blanchard, C.L., Lurmann, F.W., Roth, P.M., Jeffries, H.E., Korc, M., 1998. The use of ambient data to corroborate analysis of ozone control strategies. Manuscript.
- Cantrell, C.A., Lind, J.A., Shetter, R.E., Calvert, J.G., Goldan, P.D., Kuster, W., Fehsenfeld, F.C., Montzka, S.A., Parrish, D.D., Williams, E.J., Buhr, M.P., Westberg, H.H., Allwine, G., Martin, R., 1992. Peroxy radicals in the ROSE experiment: Measurement and theory. *Journal of Geophysical Research* 97, 20671–20686.
- Cantrell, C.A., Shetter, R.E., Calvert, J.G., Parrish, D.D., Fehsenfeld, F.C., Goldan, P.D., Kuster, W., Williams, E.J., Westberg, H.H., Allwine, G., Martin, R., 1993. Peroxy radicals as measured in ROSE and estimated from photostationary state deviations. *Journal of Geophysical Research* 98, 18355–18366.
- Cantrell, C.A., Shetter, R.E., Gilpin, T.M., Calvert, J.G., Eisele, F.L., Tanner, D.J., 1996. Peroxy radical concentrations measured and calculated from trace gas measurements in the Mauna Loa Observatory Photochemistry Experiment 2. *Journal of Geophysical Research* 101, 14653–14664.
- Cantrell, C.A., Shetter, R.E., Calvert, J.G., Eisele, F.L., Williams, E., Baumann, K., Brune, W.H., Stevens, P.S., Mather, J.H., 1997. Peroxy radicals from photostationary state deviations during the Tropospheric OH Photochemistry Experiment at Idaho Hill, Colorado, 1993. *Journal of Geophysical Research* 102, 6369–6378.
- Cardelino, C.A., Chameides, W.L., 1995. An observation-based model for analyzing ozone precursor relationships in the urban atmosphere. *Journal of the Air and Waste Management Association* 45, 161–180.
- Carter, W.L., Atkinson, R., 1989. Computer modeling study of incremental hydrocarbon reactivity. *Environmental Science and Technology* 23, 864–880.
- Chameides, W.L., Davies, D.D., Bradshaw, J., Sandholm, S., Rodgers, M., Baum, B., Ridley, B., Madronich, S., Carroll, M.A., Gregory, G., Schiff, H.I., Hastie, D.R., Torres, A., Condon, E., 1990. Observed and model-calculated  $\text{NO}_2/\text{NO}$  ratios in tropospheric air sampled during the NASA GTE/CITE-2 field study. *Journal of Geophysical Research* 95, 10235–10247.
- Chang, T.Y., Suzio, M.J., 1995. Assessing ozone-precursor relationships based on a smog production model and ambient data. *Journal of Air and Waste Management Association* 45, 20–28.
- Crawford, J., Davies, D., Chen, G., Bradshaw, J., Sandholm, S., Gregory, G., Sachse, G., Anderson, B., Collins, J., Blake, D., Singh, H., Heikes, B., Talbot, R., Rodriguez, J., 1996. Photostationary state analysis of the  $\text{NO}_2$ -NO system based on airborne observations from the western and central North Pacific. *Journal of Geophysical Research* 101, 2053–2072.
- Davis, D.D., Chen, G., Chameides, W., Bradshaw, J., Sandholm, S., Rodgers, M., Schendal, J., Madronich, S., Sachse, G., Gregory, G., Anderson, B., Barrick, J., Shipham, M., Collins, J., Wade, L., Blake, D., 1993. A photostationary state analysis of the  $\text{NO}_2$ -NO system based on observations from the subtropical/tropical North and South Atlantic. *Journal of Geophysical Research* 98, 23501–23523.
- Davis, D.D., et al., 1996. Assessment of ozone photochemistry in the western North Pacific as inferred from PEM-West A observations during the fall 1991. *Journal of Geophysical Research* 101, 2111–2134.
- Eisele, F.L., Mount, G.H., Fehsenfeld, F.C., Harder, J., Marovich, E., Parrish, D.D., Roberts, J., Trainer, M., Tanner, D., 1994. Intercomparison of tropospheric OH and ancillary trace gas measurements at Fritz Peak Observatory, Colorado. *Journal of Geophysical Research* 99, 18605–18626.
- Eisele, F.L., Tanner, D.J., Cantrell, C.A., Calvert, J.G., 1996. Measurements and steady-state calculations of OH concentrations at Mauna Loa Observatory. *Journal of Geophysical Research* 101, 14665–14679.
- Fan, S.-M., Jacob, D.J., Mauzerall, D.L., Bradshaw, J.D., Sandholm, S.T., Blake, D.R., Singh, H.B., Talbot, R.W., Gregory, G.L., Sachse, G.W., 1994. Origin of tropospheric  $\text{NO}_x$  over subarctic eastern Canada in summer. *Journal of Geophysical Research* 99, 16867–16877.
- Hauglustaine, D.A., Madronich, S., Ridley, B.A., Walega, J.G., Cantrell, C.A., Shetter, R.E., Hübler, G., 1996. Observed and model-calculated photostationary state at Mauna Loa Observatory during MLOPEX 2. *Journal of Geophysical Research* 101, 14681–14696.
- Jacob, D.J., Wofsy, S.C., 1988. Photochemistry of biogenic emissions over the Amazon Forrest. *Journal of Geophysical Research* 93, 1477–1486.
- Jacob, D.J., Heikes, B.G., Fan, S.-M., Logan, J.A., Mauzerall, D.L., Bradshaw, J.D., Singh, H.B., Gregory, G.L., Talbot, R.W., Blake, D.R., Sachse, G.W., 1996. Origin of ozone and  $\text{NO}_x$  in the tropical troposphere: a photochemical analysis of aircraft observations over the South Atlantic basin. *Journal of Geophysical Research* 101, 24235–24250.
- Johnson, G.M., 1984. A simple model for predicting the ozone concentrations of ambient air. *Proceedings of Eighth International Clean Air Conference, Melbourne, Australia, 2 May*, pp. 715–731.
- Johnson, G.M., Azzi, M., 1992. Notes on the Derivation: The Integrated Empirical Rate Model (V2.2). North Ryde, NSW, Australia, CSIRO Division of Coal and Energy Technology.
- Kleinman, L., Lee, Y.-N., Springston, S.R., Lee, J.H., Nunnermacker, L., Weinstein-Lloyd, J., Zhou, X., Newman, L., 1995. Peroxy radical concentration and ozone formation rate at a rural site in the southeastern United States. *Journal of Geophysical Research* 100, 7263–7273.
- Kleinman, L.I., Daum, P.H., Lee, J.H., Lee, Y.-N., Nunnermacker, L.J., Springston, S.R., Newman, L., Weinstein-Lloyd, J., Sillman, S., 1997. Dependence of ozone production on NO and hydrocarbons in the troposphere. *Geophysical Research Letters* 24, 2299–2302.
- Kleinman, L.I., Daum, J.H., Lee, Y.-N., Lee, J., Weinstein-Lloyd, Springston, S.R., Buhr, M., Jobson, B.T., 1998. Photochemistry of  $\text{O}_3$  and related compounds over southern Nova Scotia. *Journal of Geophysical Research* 103, 13519–13529.
- Leighton, P.A., 1961. *Photochemistry of Air Pollution*. Academic Press, New York.
- Lin, X., Trainer, M., Liu, S.C., 1988. On the nonlinearity of the tropospheric ozone production. *Journal of Geophysical Research* 93, 15879–15888.
- Liu, S.C., Trainer, M., Carroll, M.A., Hübler, G., Montzka, D.D., Norton, R.B., Ridley, B.A., Walega, J.G., Atlas, E.L., Heikes, B.G., Huebert, B.J., Warren, W., 1992. A study of the

- photochemistry and ozone budget during the Mauna Loa Observatory Photochemistry Experiment. *Journal of Geophysical Research* 97, 10463–10471.
- McKeen, S.A., Mount, G., Eisele, F., Williams, E., Harder, J., Goldan, P., Kuster, W., Liu, S.C., Baumann, K., Tanner, D., Fried, A., Sewell, S., Cantrell, C., Shetter, R., 1997. Photochemical modeling of hydroxyl and its relationship to other species during the Tropospheric OH Photochemistry Experiment. *Journal of Geophysical Research* 102, 6467–6493.
- Milford, J., Gao, D., Sillman, S., Blossey, P., Russell, A.G., 1994. Total reactive nitrogen ( $\text{NO}_y$ ) as an indicator for the sensitivity of ozone to  $\text{NO}_x$  and hydrocarbons. *Journal of Geophysical Research* 99, 3533–3542.
- Parrish, D.D., Trainer, M., Williams, E.J., Fahey, D.W., Hübler, G., Eubank, C.S., Liu, S.C., Murphy, P.C., Albritton, D.L., Fehsenfeld, F.C., 1986. Measurements of the  $\text{NO}_x - \text{O}_3$  photostationary state at Niwot Ridge, Colorado. *Journal of Geophysical Research* 91, 5361–5370.
- Poppe, D., Zimmermann, J., Bauer, R., Brauers, T., Brüning, D., Callies, J., Dorn, H.-P., Hofzumahaus, A., Johnen, F.-J., Khedim, A., Koch, H., Koppmann, R., London, H., Müller, K.-P., Neuroth, R., Plass-Dülmer, C., Platt, U., Rohrer, F., Röth, E.P., Rudolph, J., Schmidt, U., Wallasch, M., Ehhalt, D., 1994. Comparison of measured OH concentrations with model calculations. *Journal of Geophysical Research* 99, 16633–16642.
- Ridley, B.A., Madronich, S., Chatfield, R.B., Walega, J.G., Shetter, R.E., Carroll, M.A., Montzka, D.D., 1992. Measurements and model simulations of the photostationary state during the Mauna Loa Observatory Experiment: implications for radical concentrations and ozone production and loss rates. *Journal of Geophysical Research* 97, 10375–10388.
- Sillman, S., Logan, J.A., Wofsy, S.C., 1990. The sensitivity of ozone to nitrogen oxides and hydrocarbons in regional ozone episodes. *Journal of Geophysical Research* 95, 1837–1851.
- Sillman, S., 1995. The use of  $\text{NO}_y$ , HCHO,  $\text{H}_2\text{O}_2$  and  $\text{HNO}_3$  as indicators for ozone- $\text{NO}_x$ -hydrocarbon sensitivity in urban locations. *Journal of Geophysical Research* 100, 14175–14188.
- Sillman, S., He, D., Cardelino, C., Imhoff, R.E., 1997. The use of photochemical indicators to evaluate ozone -  $\text{NO}_x$  - hydrocarbon sensitivity: case studies from Atlanta, New York and Los Angeles. *Journal of Air Waste Management Association* 47, 1030–1040.
- Sillman, S., He, D., Pippin, M., Daum, P.H., Lee, J.H., Kleinman, L., Weinstein-Lloyd, J., 1998. Model correlations for ozone, reactive nitrogen and peroxides for Nashville in comparison with measurements: implications for  $\text{O}_3$ - $\text{NO}_x$ -hydrocarbon chemistry. *Journal of Geophysical Research* 103, 22629–22644.
- Staffelbach, T., Neftel, A., Blatter, A., Gut, A., Fahrni, M., Stähelin, J., Prévôt, A., Hering, A., Lehning, M., Neisinger, B., Bäumle, M., Kok, G.L., Dommen, J., Hutterli, M., Anklin, M., 1997a. Photochemical oxidant formation over southern Switzerland 1. Results from summer 1994. *Journal of Geophysical Research* 102, 23345–23362.
- Staffelbach, T., Neftel, A., Horowitz, L.W., 1997b. Photochemical oxidant formation over southern Switzerland 2 Model results. *Journal of Geophysical Research* 102, 23363–23373.
- Tonnesen, G.S., Dennis, R.L., 1997a. Analysis of indicator species to assess odd oxygen production sensitivity to hydrocarbon and nitrogen oxides in photochemical models. *Journal of Geophysical Research*, submitted for publication.
- Tonnesen, G.S., Dennis, R.L., 1997b. An analysis of radical propagation efficiency to derive combinations of long-lived species as indicators of ozone sensitivity to  $\text{NO}_x$  and hydrocarbons. *Journal of Geophysical Research*, submitted for publication.
- Trainer, M., Parrish, D.D., Buhr, M.P., Norton, R.B., Fehsenfeld, F.C., Anlauf, A.G., Bottenheim, J.W., Tang, Y.Z., Wiebe, H.A., Roberts, J.M., Tanner, R.L., Newman, L., Bowersox, V.C., Meagher, J.F., Olszyna, K.J., Bailey, E.M., Dorris, S., Rogers, M.O., Demerjian, K., 1993. Correlation of ozone with  $\text{NO}_y$  in photochemically aged air. *Journal of Geophysical Research* 98, 2917–2925.